Universal Descreening Technique Via Wavelet Analysis

Jiebo Luo
Imaging Research
Eastman Kodak Company
Rochester, NY 14650
luo@image.kodak.com

Ricardo de Queiroz
Digital Imaging Technology Center
Xerox Corporation
Webster NY, 14580
queiroz@wrc.xerox.com

Zhigang Fan
Zhigang_Fan@wb.xerox.com

ABSTRACT

In this paper, a novel wavelet-based approach to recover continuous tone images from halftone images is presented. Wavelet decomposition of the halftone image facilitates a series of spatial and frequency selective processing to preserve most of the original image contents while eliminating the halftone noise. Furthermore, optional non-linear filtering can be applied as a post-processing stage to create the final aesthetic contone image. This approach lends itself to practical applications since it is independent of parameter estimation and hence universal to all types of halftoned images, including those obtained by scanning printed halftones.

Keywords: halftone, inverse halftoning, wavelet, descreening, nonlinear smoothing, noise attenuation

1 INTRODUCTION

Halftoning is a quantization process which reduces bit-depth of a digital image while trying to maintain the gray scale appearance.[1–3] The main applications of halftoning are printing and displaying, where continuous-tone pictures are reproduced on binary output devices.

Descreening, or retrieving a continuous-tone image from a halftone, is a problem not only of great theoretical interest as an ill-posed inverse problem, but also of significant practical usage. A halftone image usually has very different characteristics than a continuous-tone image, which make it hostile to many common image processing procedures. For example, compression would be inefficient due to the rich high frequency noise in halftones. Scaling, rotation and rescreening would be unacceptable due to the introduction of strong Moiré effects. Tone correction and enhancement would also be impossible due to the limited bit depth of the halftones. As a result, descreening is usually the first step for any halftone image processing.

Most digital halftoning methods can be classified into three categories: ordered dithering, error diffusion and optimization-based. In ordered dithering, the continuous-tone image is quantized with a periodical threshold matrix.[1–3] The organization of the threshold matrix determines the appearances of the halftone images. They may be composed of dots of different sizes (clustered dot screening), or scattered pixels (dispersed dot screening).[3,4] The stochastic screening methods reported in[5] can also be viewed as special cases of dispersed dots. They typically use large threshold matrices, which are designed to produce halftones with "blue noise" characteristics. Error diffusion is an adaptive process.[6] The quantization of a pixel is performed on the modified input, which is the combination of the input signal and the quantization errors *diffused* from neighboring processed pixels. The errors are propagated in a weighted manner. The weighting coefficients control the appearance of the resulting halftone. Optimization methods are iterative search algorithms which try to minimize some cost function associated with the pixel arrangement.[7,8]

The spectrum of the halftoning noise is largely high-pass in nature. Nevertheless, it differs significantly for various processes. The noise energy of amplitude modulated (AM) methods such as clustered dot screening, are concentrated

in a few spikes at screen frequencies and their harmonics.[9] The spectrum structure is relatively insensitive to the changes of input values. On the other hand, the noise spectrum of most frequency modulation (FM) techniques, such as error diffusion, stochastic screening and optimization methods are usually smooth and continuous. Furthermore, they are typically "blue", i.e., contain less low-frequency energy. The cut-off frequencies of these methods, however, depend highly on the input gray level. They are higher for mid-tone values and lower for high-lights and shadow values. Bayes dispersed dot screening[4] exhibits a mixed behavior. It belongs to FM methods and its frequency response is highly input-dependent. However, its spectrum contains strong peaks, similar to clustered dots.

The statistics of images differ significantly between orthographical halftones and scanned ones. The former refer to the halftones created digitally and acquired in a digital form, while the latter refer to the halftones printed and then obtained through a scanner. The descreening of scanned halftone is particularly useful for many practical applications. As a first order approximation, the scanned halftone can be considered as a low-pass filtered version of the original halftone. The halftone effects are usually reduced. The degree of the weakening depends on the relative resolutions of the scanning versus the printing. The lower the scanning resolution, the less the halftoning effects, and vice versa. In the orthographic halftones, the halftone value (black or white) of each pixel reveals a possible range of the input value (or modified input value for the error diffusion) of the pixel. This provides important clues for descreening. However, this benefit usually does not exist for scanned halftones, as they lack the perfect registration typical of orthographic halftones.

Since halftoning noise is mainly concentrated in high frequency, the screens can be effectively removed by low-pass filtering. However, the smoothing tends to blur edges and destroy fine details in the original image. Many different methods were reported to improve descreening.[10–22] They can be roughly divided into two groups. The first kind of approach is to treat descreening as a constrained optimization problem.[10–16]

Perfect registration and availability of halftoning parameters are assumed. The possible range of input (or modified input for error diffusion) is then utilized as constraints. The optimization can be performed using projection onto convex sets (POCS),[10] logical filtering,[11] iterative filtering,[12] quadratic programming,[13] or other techniques.[14–16] The second class of methods is based on edge-preserving smoothing. It includes binary permutation filtering,[17] sigma filtering,[18] orientation sensitive filtering,[19] adaptive filtering,[20] statistical smoothing,[12] and smoothing using vector quantization lookup tables.[21] There are also algorithms combining smoothing approaches and constrained optimization approaches.[22]

Most of the descreening methods are designed for a particular halftoning process. Some of them are tuned or trained for a particular set of halftone parameters. They fail or perform poorly when the condition changes. They also often assume *a priori* knowledge of halftoning parameters, such as screening frequencies, threshold matrices, or error diffusion weights. However, in real applications, the original halftoning methods and its associated parameters are generally unknown. A robust estimation is usually difficult to achieve. Moreover, often the image is obtained by scanning halftone material.

Our novel wavelet-based universal approach is independent of the halftoning method and is also applicable to scanned halftones. It is facilitated by the wavelet transform or by overcomplete subband representations in such a way that the image is analyzed at multiple resolutions and possible halftone patterns are attenuated, without making any assumption about the halftoning method used to create the halftone image.

2 WAVELETS AND HIERARCHICAL FILTERING

Subband transforms and filter banks are useful tools to separate an input signal into several subband signals.[23] These subband signals contain fractions of the input spectrum. In a hierarchical association of M-channel filter banks the original image O is split into M subbands $S(0,i)$ as in Fig. 1(a). The low-pass subband $S(0,0)$ is further decomposed into M subbands $S(1,i)$ and the process is repeated a number of times, always decomposing the low-pass subband $S(j,0)$. Every time the process is repeated, subbands with lower frequency contents are generated. One attractive property of subband decompositions is the fact that different subbands convey information regarding different frequency bands. Inside a subband, different coefficients represent different spatial locations.

The concept of a *tree* relating the subband coefficients emerges from the hierarchical relations among the subbands. The *parent* of a coefficient is a coefficient in a subband with the same orientation as its own, at lower frequency, occupying the same relative spatial position. Fig. 1(b) illustrates the relation. The use for a *tree* notation will be made clear later on.

For image processing, a common approach is to associate 2-channel filter banks, composed of low- and high-pass filters, and yielding a 4-channel system. This 2D separable implementation is shown in Fig. 2. The low- and high-pass filters (LPF and HPF, respectively) may have their output decimated by a factor of two.[23] However, in overcomplete and pyramidal expansions this may not be the case as we will discuss later on. The hierarchical connection of the 2D 4-channel stages generates the discrete wavelet transform (DWT).

In the preferred way to implement the DWT, the filters' output is decimated and the resulting decomposition along with parent-descendant relationships are illustrated in Fig. 3. The horizontal subband is obtained by low-pass filtering in the vertical direction and by high-pass filtering in the horizontal direction. The opposite configuration yields the vertical subband, while the diagonal subband is a product of high-pass filtering in both directions. The low-pass filtered signal (in both directions) is fed to another filter bank stage, therefore generating new subband levels. The subbands at level n are labeled Vn, Hn, or Dn, for the vertical, horizontal, and diagonal orientations, respectively. At the end of the recursion, we obtain a low-pass signal denoted as "LP", which is also called the base band.

3 DESCREENING METHODOLOGY

We propose a descreening scheme composed of sequential stages: (i) subband decomposition; (ii) noise attenuation in non-edge areas (iii) oriented filtering; (iv) inverse subband recomposition; and (v) an optional non-linear edge-preserving post-filtering stage. In the following, each of these stages will be discussed in detail.

3.1 Wavelet Decomposition and Its Inverse

The halftone image is first decomposed into different frequency subbands using the DWT with separable filter banks[23] as in Figs. 2 and 3. While the energy of the halftoning process resides primarily in the high frequency subbands, the low frequency subbands contain most of the signal energy. The high frequency subbands, where the signal energy and halftoning energy are heavily mixed together, contain signal energy corresponding to important edge information. It has been recognized that the key to the success of the descreening is how to differentiate high frequency image contents from the halftone noises. In the past, frequency domain oriented descreening approaches, i.e., lowpass filtering based approaches, haven't been very successful due to the heavy mixture of halftone noises with high frequency image contents such as edges and texture. While an increasing amount of halftone noise can be removed by applying lowpass filtering with lower cutoff frequency, the increasing amount of loss of high frequency image contents inevitably cause more severe degradation of the reconstructed contone image.

Wavelet decomposition facilitates selective processing in both frequency and space domains. After the wavelet decomposition, a space frequency representation is obtained. At each given level, except the base band, there are three high frequency subband images corresponding to horizontal, vertical, and diagonal orientations. There are several properties that are significant and will be exploited by the proposed descreening approach:

- Each high frequency subband image has a distinctive orientation.
- Each high frequency subband image is composed of coefficients corresponding to similar frequency components at different locations.
- Each high frequency subband coefficient is part of a hierarchical tree

  composed of coefficients corresponding to different frequency components in the same spatial neighborhood.

The inverse DWT reconstructs the signal from the subbands. Processing in the DWT domain is depicted in Fig. 4. In this figure, it is shown the subbands of the wavelet decomposition before and after they are processed by noise attenuation techniques that will be discussed next.

3.2 Noise Attenuation (Frequency Correlation)

There exists a hierarchical relationship among the amplitude of the subbands samples at different resolution levels, but same spatial location. For a given coefficient (parent), there are four coefficients (children) at the same spatial location in the subband of the same orientation at the next finer resolution. This relationship is illustrated in Fig. 3. It is found that in general the magnitudes of the descendants are non-increasing with respect to their ancestors. Note that this observation is particularly true if a gain factor of 2 is applied each time a subband is further decomposed (in order to ensure the energy conservation in the wavelet transform). Subbands at lower resolutions have gone through more stages o f filtering, therefore they generally have larger dynamic ranges. In other words, the power spectrum of the image signal commonly decays as the frequency increases. This assumption has been successfully applied for image coding.[24] The violation of this constraint is often an indication of the presence of halftoning energy. Therefore, we clip the coefficients in the high frequency subbands so that their magnitudes are not larger than the magnitude or weighted magnitude of their parents. Weights may vary from level to level and the clipping process can be made adaptive (more conservative over edges and more aggressive otherwise).

3.3 Intraband Filtering (Spatial Correlation)

An important part of descreening is to preserve the edges to the maximum extent. In the first step of noise attenuation, we did not consider edges in a spatial context. Moreover, there are still significant halftone noises in the vicinity of edges in comparison with the subband images of the original contone image.

In order to further reduce the halftone noise near edges, one must first locate the edges. Fortunately, within the framework of wavelet decomposition, edge contents have been decomposed into well separated subband images with respect to frequency, location, and orientation. Each subband image contains edge components primarily along its orientation. Vertical subbands have vertical high frequency components which are commonly caused by objects whose edges are displaced horizontally. Similarly, vertically oriented edges may appear in the horizontal subbands. Diagonal subbands contain residual components. Therefore, it is intuitive that if we low-pass filter the subband images along specific orientations we might remove noisy components and not degrade sharp edges extensively. In particular, a one-dimensional lowpass filtering L-point filter can be applied to both horizontal and vertical subbands, i.e., a horizontal low-pass filter is applied to the vertical subband and vice-versa, while an X-shaped lowpass filter is applied to the diagonal subbands.

Oriented filtering can be performed adaptively with respect to the resolution scale of each subband, e.g., the length parameter L should be reduced monotonically going into lower frequency subbands. Furthermore, estimates of the screen parameters can be used in selecting the appropriate filters in terms of the length parameter L. Filtering can be implemented as convolution using the following types of square kernels for vertical, horizontal, and diagonal subbands:

horizontal	vertical	diagonal
$0\ b_1\ 0$	$0\ \ 0\ \ 0$	$b_2\ 0\ b_2$
$0\ a_1\ 0$	$b_1\ a_1\ b_1$	$0\ a_2\ 0$
$0\ b_1\ 0$	$0\ \ 0\ \ 0$	$b_2\ 0\ b_2$

where $a_1 = \alpha$, $b_1 = (1-\alpha)/2$, $a_2 = 3\alpha/5$, $b_2 = (5-3\alpha)/20$, and α is a bandwidth control parameter for the filters. As an alternative approach to oriented filtering, explicit edge estimation can also be implemented to guide the filtering.

3.4 Nonlinear Postfiltering

The reconstructed contone image from inverse wavelet recomposition may still suffer from some artifacts, such as ringing and blotchiness, due to the loss of (high-frequency) signal information. The most observable is the ringing artifact around prominent edges. Ringing effect is frequently encountered in wavelet-based image processing due to the loss of high frequency components. In this case, it is caused by partial loss of high frequency components although we are able to capture most significant portion of the edge contents through the previous selective noise attenuation processes within the subbands.

The reconstructed contone image is preferably enhanced in the *original* space domain using a nonlinear filtering with the spatial smoothness constraints modeled by a discontinuous image prior model.[25] In this study, we choose to perform a postfiltering to enhance the contone image in the *original* space domain to take advantage of the prior arts in this regard. The postfiltering is accomplished with the incorporation of a Markov random field (MRF), in particular the Huber Markov random field (HMRF),[27] which has been used to various image smoothing applications.[28,29] Markov random field, in particular Gibbs random field (GRF) has been widely used to model the neighborhood constraints in images in various image processing and computer vision tasks.[30] The main advantage of using a GRF instead of an MRF is that it is convenient to parameterize a GRF using a Gibbs potential function and a proper neighborhood system.[30,29] In general, a GRF image prior model, i.e., the constraints among neighboring pixels, is enforced by

$$p(x) \propto \exp\{-\sum_{c \in C} V_c(x)\} \tag{1}$$

where $p(x)$ denotes the *a priori* probability of the random field, i.e., image x, and $V_c(x)$ is the potential function defined upon the neighborhood system C ($c \in C$ denotes a local neighborhood).

There are a number of convex potential functions which have been used to enforce image smoothness constraint within the framework of Gibbs random field.[25,29] Convex functions are often desired because the convergence of a convex constrained problem is always guaranteed if solutions do exist, and it can also be optimized efficiently due to fast convergence. More importantly, convex potential functions with smooth transition, i.e., with good continuity properties, result in desired continuity in the image. However, there may be significant discontinuities such as edges in the image. In other words, image is a *non-stationary* random field. As shown in Fig. 5, the quadratic Gaussian prior model (GMRF), which corresponds to MSE (mean square error) criterion, is unable to differentiate these discontinuities or the outliers of the model and its linear lowpass filtering nature tends to blur image edges and other details excessively and indiscriminately.[29] In other words, such a stationary model is inadequate to characterize the statistics of images due to their non-stationary nature. Therefore, discontinuous (in terms of first or higher order derivatives) functions are more desirable because they are capable of being adaptive to discontinuities, e.g., the Huber minimax function given by:

$$\rho_T(x) = \begin{cases} x^2, & |x| \le T \\ T^2 + 2T(|x| - T), & |x| > T \end{cases} \tag{2}$$

where T is a threshold and x denotes the difference between neighboring pixels. A major advantage of the HMRF model over other types of GRF models for image restoration is its ability to switch the penalty on discontinuities according to the difference of gray level between the current pixel and its neighbors. The quadratic segment of the function imposes least mean square smoothing of the artifacts when the local variation is below T. On the other hand, the linear segment of the function enables the preservation of image details by allowing large discontinuities in the image with a much lighter penalty. In terms of implementation, the HMRF model is advantageous over other discontinuous MRF models[25] in making the computation more efficient because only linear operations are involved in the optimization where gradient, in this case a piecewise linear function, is commonly used.

Other edge-preserving filtering methods (such as σ-filter[31] based filtering), though not within the framework of GRF-based estimation, are also applicable at this stage. A σ-filter behaves mostly like a linear convolution filter, except for just including samples whose levels are within $\pm\sigma$ levels from the center pixel. Thus,

$$\tilde{x} = mean\{x_{ij} | ij \in W, |x - x_0| \le \sigma\} \tag{3}$$

where x_0 is the value of the center pixel and W is a region neighboring x_0. In a σ-filter, the estimate of the smoothed

value $\tilde{x}$ is the local running average of the neighboring pixels, within a specified local window, which have similar values. Thus, sharp edges are not blurred by the process.

In practice, the best enhancement results are obtained by sequentially processing the reconstructed contone image with HMRF-based filtering and σ-filter based filtering. It can be understood that the HMRF-based filtering provides smooth transition while preserving edges, and a subsequent σ-filter based filtering has the effect to further clean and sharpen the prominent edges. Note that the order of applying these two types of nonlinear filtering matters. After the nonlinear postfiltering, both the ringing and the blotchiness caused by remaining halftone noises are effectively removed.

4 EXPERIMENTAL RESULTS

We generated examples using a 4-level DWT based on Johnston's 16-tap filters,[32] although other filters may be used as well.[23] The 400×400 pel image shown in Fig. 6(a) is a 3×3 clustered dot halftone. The contone image was reconstructed by applying uniform-weight clipping and oriented filtering ($\alpha = 1/3$) to the subbands at 3 topmost levels. Also, a combination of HMRF-based filter and σ-filter is used as post processing. The result is shown in Fig. 6(b). For illustration purposes, the 4-level wavelet transform of the halftone image is shown in Fig. 6(c). After clipping and oriented filtering, the subbands are shown in Fig. 6(d).

To demonstrate the robustness of the algorithm we repeat the experiment for other types of halftones using same parameters. An error diffused image is shown in Fig. 7(a) and its reconstructed contone version is shown in Fig. 7(b). Furthermore, the method can also be used for scanned material. We printed an image using 4×8 cluster dots in a 300 dpi laser printer and scanned the printed material at 200 ppi. The scanned image is shown in Fig. 7(c), while its descreened version is shown in Fig. 7(d). In the case of error diffusion, using the standard "lena" image, the quality of the recovered contone image, both subjectively and objectively, is among the best published.

Non-linear filters such as the HMRF- or σ-based approaches can be applied at this stage to further clean the image and sharpen edges. The effect of the detail-preserving nonlinear post-filtering can be appreciated by comparing the final contone images with the contone images obtained right after the inverse DWT, without any post-processing stage. The images referring to Fig. 6(a)(b) and to Fig. 7(a)(b) are shown in Fig. 8.

5 CONCLUSIONS AND FUTURE DIRECTIONS

We have presented a novel wavelet-based approach to recover continuous tone images from halftone images. A series of spatial and frequency selective processing is applied to the subbands resulting from a wavelet decomposition of the halftone image. Such a processing is designed to preserve most of the original image features while eliminating the halftone noise. In addition, non-linear filtering can be applied as a post-processing stage to further clean the halftone noise patterns that might have survived the DWT-domain processing. The proposed wavelet-based descreening technique may not be the best for a given type of halftone pattern, but it has been successfully applied to virtually all types of halftoning methods. Knowledge of the halftone process is not required. This approach lends itself to practical applications since it is independent of parameter estimation and hence is virtually universal to most types of halftoning techniques, including those obtained by scanning halftoned material. A forthcoming paper will explain in more details the proposed algorithm as well as its extension to encompass overcomplete wavelet decomposition.

REFERENCES

[1] J. C. Stoffel and J. F. Moreland, "A survey of electronic techniques for pictorial image representation," *IEEE Trans. on Communications,* vol. COM-29, pp. 1898–1925, Dec. 1981

[2] R. A. Ulichney, *Digital Halftoning,* Cambridge, MA, MIT Press, 1987.

[3] P. G. Roetling and R. P. Loce, "Digital Halftoning," Chap. 10, in *Digital Image Processing Methods*, E. Dougherty Ed., Marcel Dekker, New York, NY, 1994.

[4] B. E. Bayer, "An optimum method for two-level rendition of continuous-tone pictures," *Proc. of IEEE Intl. Conf. on Communications*, vol. 1, pp 26-11, 26-15, 1973.

[5] T. Mitsa, K. J. Parker, "Digital Halftoning with a blue noise mask," *Proc. SPIE/IS&T Symposium on Electronic Imaging*, San Jose, 1991.

[6] R. Floyd, L. Steinberg, "An adaptive algorithm for spatial grey scale," *Proc. SID,* Vol. 17, No. 2, p. 75, 1976.

[7] M. Analoui and J. Allebach, "Model based halftoning using direct binary search," *Proc. SPIE Conf. Human Vision, Vis. Proc. and Dig. Display III*, San Jose, Feb. 1992.

[8] T. N. Pappas, D. L. Neuhoff, "Least squares model based halftoning," *Proc. SPIE Conf. Human Vision, Vis. Proc. and Dig. Display III*, San Jose, Feb. 1992.

[9] D. Kermisch and P. G. Roetling, "Fourier spectrum of halftone images," *Journal of the Optical Society of America*, vol. 65, pp. 716–722, June 1975.

[10] M. Analoui and J. Allebach, "New results on reconstruction of continuous-tone from halftone," *Proc. IEEE Intl. Conf. Acoust. Speech Sig. Proc.*, vol. 3, pp. 313–316, San Francisco, CA,1992.

[11] Z. Fan, "Retrieval of images from digital halftones," *Proc. Intl. Symp. on Circuits and Systems,* pp. 313-316, May 1992.

[12] P. W. Wong, "Inverse halftoning and kernel estimation for error-diffusion," *IEEE Trans. Image Processing,* Vol. 4, No. 4, pp. 486-498, 1995.

[13] S. Hein and A. Zakhor, "Halftone to continuous-tone conversion of error-diffusion coded images," *IEEE Trans. Image Processing,* Vol. 4, No. 2, pp. 208-216, 1995.

[14] C. M. Miceli and K. J. Parker, "Inverse Halftoning," *J. of Electronic Imaging* Vol. 1, No. 2, pp. 143-151, Apr., 1992.

[15] S. Schweitzer and R. Stevenson, "Bayesian approach to inverse halftoning," *Proc. SPIE Conf. Human Vision, Vis. Proc. and Dig. Display IV*, Proc. SPIE 1913, pp. 282–292, 1993.

[16] P. Roetling, "Unscreening of stored digital halftone images," U.S. Patent 4,630,125.

[17] Y. Kim, G. R. Arce, and N. Grabowski, "Inverse halftoning using binary permutation filters,' *Proc. IEEE Trans. Image Processing,* vol. 4, pp. 1296–1311, Sep. 1995.

[18] Z. Fan, "Image processing system and method with improved reconstruction of continuous tone images from halftone images including those without a screen structure", US patent 5,243,444.

[19] P. Roetling, "Image processing system and method employing adaptive filtering to provide improved reconstruction of continuous tone images from halftone images including those without a screen structure," U.S Patent 5,343,309.

[20] L. M. Chen and H. M. Hang, "Inverse halftone for monochrome pictures," *Proc. IEEE Intl. Conf. on Image Processing,* pp. 1020–1026, 1994.

[21] M. Y. Ting and E. Riskin, "Error-diffused image compression using a halftone to gray scale decoder and predictive pruned tree-structured VQ," *Proc. SID*, May 1993.

[22] Z. Fan, "Unscreening using a hybrid filtering approach," *Proc. IEEE Intl. Conf. on Image Processing,* vol III, pp. 351–354, 1996.

[23] G. Strang and T. Nguyen, *Wavelets and Filter Banks*, Wellesley-Cambridge, Wellesley, MA, 1996.

[24] J. M. Shapiro, "Embedded image coding using zerotrees of wavelet coefficients," *IEEE Trans. Signal Processing,* vol. 41, pp. 3445-3462, Dec. 1993.

[25] S. Z. Li, "Discontinuous MRF prior and robust statistics: a comparative study", *Image and Vision Computing",* vol. 13, no. 3, pp. 227-233, April 1995.

[26] J. Luo and C. W. Chen and K. J. Parker, "On the modeling of subband coefficients in wavelet image coding with clustering-based adaptive quantization", *Proc. of 1996 Conf. on Information Sciences and Systems,* March 1996, Princeton, NJ.

[27] P. J. Huber, *Robust statistics*, Wiley, New York, 1981.

[28] R. L. Stevenson et al., "A nonlinear filtering structure for image smoothing in mixed noise environments," *Journal of Mathematical Imaging and Vision,* vol. 2, no. 3, pp. 137-154, Nov. 1992.

[29] J. Luo and C. W. Chen and K. J. Parker, "On the application of Gibbs random field in image processing: from segmentation to enhancement", *Journal of Electronic Imaging,* vol. 2, no. 2, pp. 189-198, April 1995.

[30] R. Chellappa and A. Jain, *Markov Random Fields-Theory and Applications*, Academic, New York, 1993.

[31] J. Lee, "Digital image smoothing and the σ-filter", *Computer Vision, Graphics and Image Processing,* vol. 24, pp. 255-269, 1983.

[32] J. D. Johnston, "A filter family designed for use in quadrature mirror filter banks," *Proc. of Intl. Conf. on Acoustics, Speech and Signal Processing,* pp. 281-284, 1980.

[33] Z. Xiong, K. Ramchandran and M. Orchard, "Inverse halftoning using wavelets", *Proc. of Intl. Conf. on Image Processing,* Lausanne, CH, Vol. I, pp. 569–572, 1996.

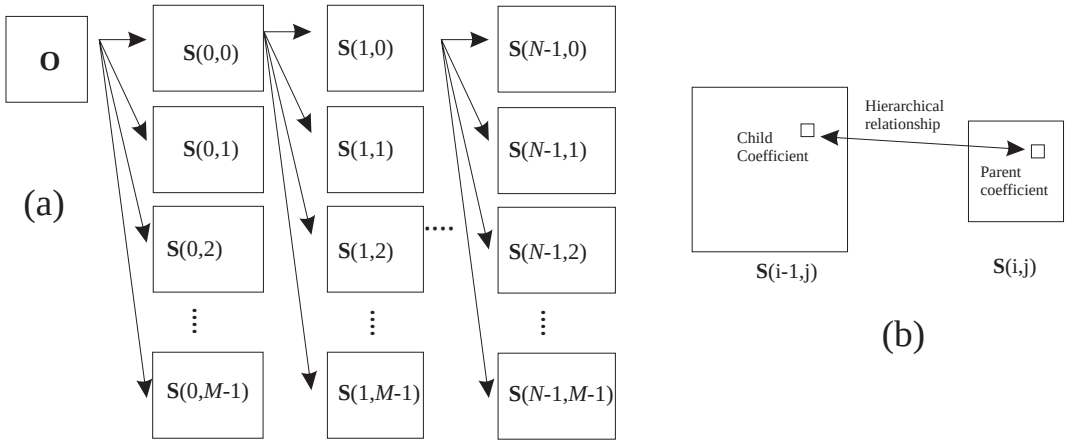

Figure 1: The subband decomposition and the parent-descendent relationship.

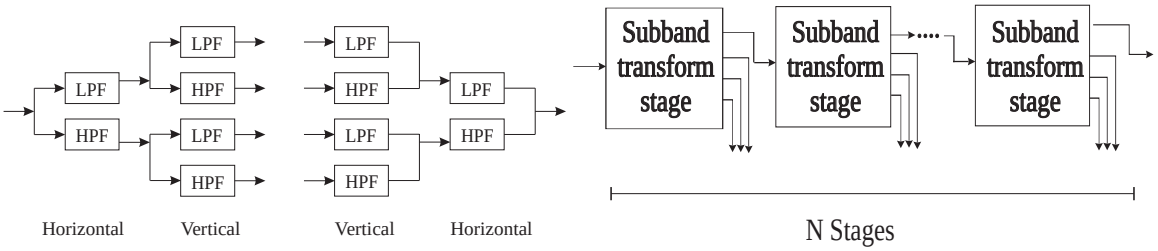

Figure 2: The 2D 4-band filter bank made of 1D 2-channel filter banks. The hierarchical association of these filter banks generates the DWT.

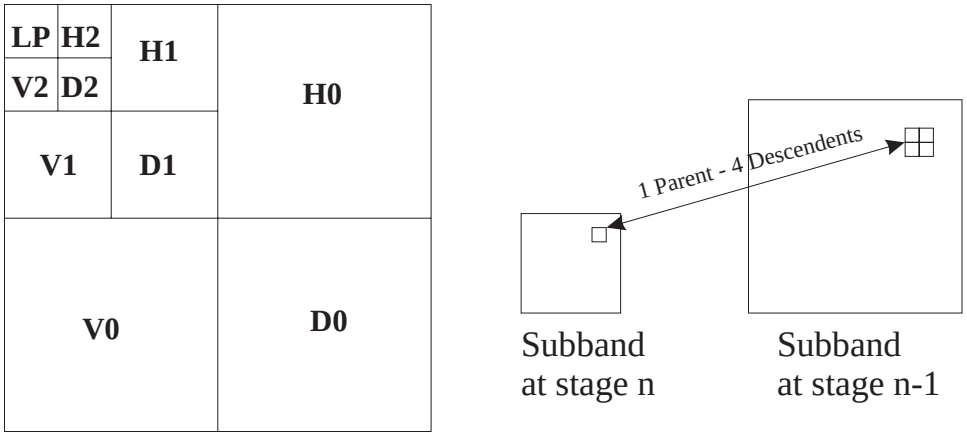

Figure 3: The DWT decomposition and its parent-descendent relationship.

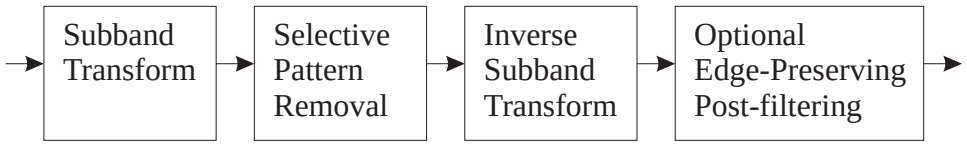

Figure 4: Basic diagram for descreening facilitated by the DWT.

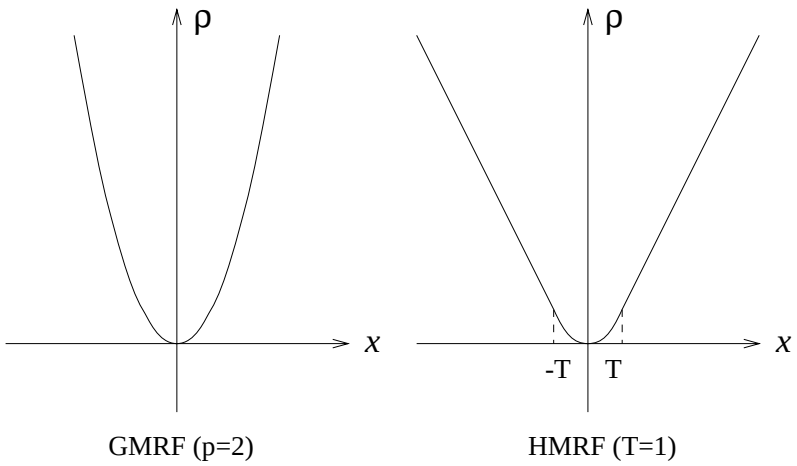

Figure 5: Quadratic potential function and the Huber minimax potential function.

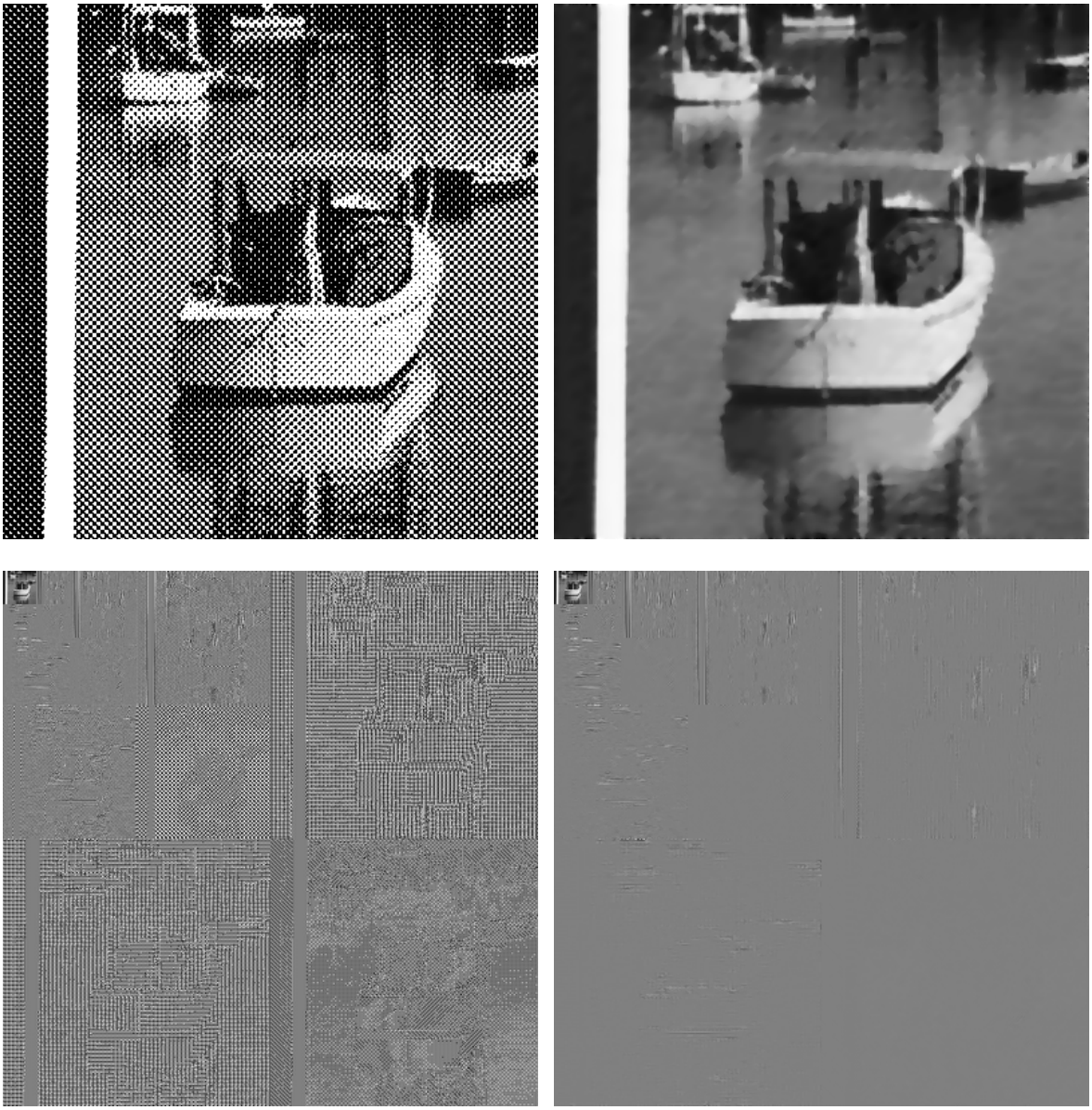

a	b
c	d

Figure 6: Halftone image (a) and its reconstructed contone version (b). Image size is 400×400 and halftoning method employs $3\times$ 3 clustered dots. The wavelet transform of the halftone image is shown in (c) which is processed (cleaned) generating the image in (d).

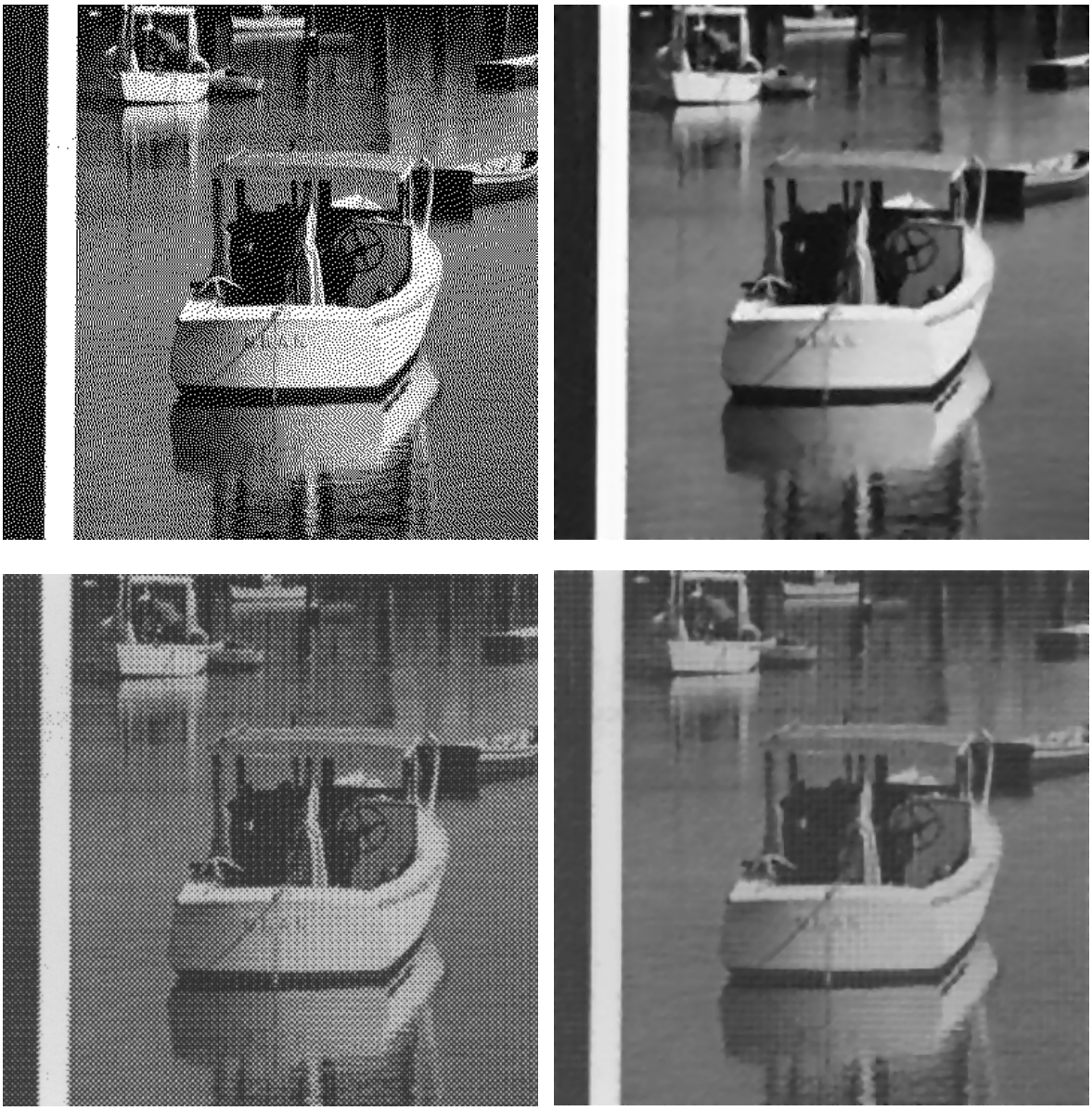

a	b
c	d

Figure 7: Reconstructed contone versions from halftone images. (a) Error diffusion halftone and (b) its reconstructed version. (c) Scanned halftone and (d) its reconstructed version.

a b

Figure 8: Reconstructed raw contones from cleaned subband images without post-filtering. (a) from error diffusion halftone and (b) from clustered dots halftone.